Direct Molecular Dynamics Using Quantum Chemical Hamiltonians: C60 Impact on a Passive Surface

ARTICLE *in* THE JOURNAL OF PHYSICAL CHEMISTRY A · JUNE 2001

Impact Factor: 2.69 · DOI: 10.1021/jp011394z

4 AUTHORS, INCLUDING:

Rodney J. Bartlett
University of Florida

663 PUBLICATIONS **39,827** CITATIONS

SEE PROFILE

Direct Molecular Dynamics Using Quantum Chemical Hamiltonians: C_{60} Impact on a Passive Surface

Ya-Wen Hsiao, Keith Runge, Marshall G. Cory, and Rodney J. Bartlett*

Quantum Theory Project and Departments of Physics and Chemistry, University of Florida, Gainesville, Florida 32611-8435

Received: April 12, 2001; In Final Form: May 18, 2001

Quantum chemical Hamiltonians of the semiempirical type potentially provide a more reliable description of a potential energy surface for large scale molecular dynamics than does the tight-binding (TB) Hamiltonian, a reparametrized extended Hückel Hamiltonian including a short range repulsion. Their performance is tested here and compared with results from TB simulations. The methods considered are from the zero differential overlap family of semiempirical Hamiltonians, these are the intermediate neglect of differential overlap (INDO) method and three parametrizations of the neglect of differential diatomic overlap (NDDO) method, AM1, PM3, and MNDO. The collision of the C_{60} molecule with a passive surface at two collision energies is the test problem, where the higher energy leads to shattering of the molecule. The NDDO Hamiltonians are found to give a better qualitative description than the INDO Hamiltonian at both energies and further studies to reparametrize the NDDO form for direct MD are indicated.

Introduction

Molecular dynamics (MD) simulation is a useful tool for probing physical and chemical processes in large systems. The simulation follows nuclear trajectories determined by Newton's law of motion, and hence information about the potential energy of the system is needed to obtain forces. For small systems, one may obtain the potential energy surface using accurate ab initio Hamiltonians, and then proceed with MD simulations. For extended systems, direct MD, where forces are calculated on the fly, is more desirable and empirical potential energy functions and the tight-binding (TB) Hamiltonians have been widely used in this connection. Both empirical potential energy functions and TB Hamiltonians rely upon a set of parameters tuned to reproduce materials properties in order to describe the atomic interactions in the systems considered. A fundamental difference between the two procedures is that the TB Hamiltonian approach is a simplified quantum mechanical description while the empirical functions use forms derived from the theory of molecular interactions and not quantum chemical methods.

The tight-binding method, which is a reparametrized Hückel molecular orbital method[1] of computational chemistry including a short range repulsion, is the simplest frequently used semiempirical molecular orbital method. It contains a few nonzero empirical one-electron parameters that distinguish among the various parametrizations of the Hückel Hamiltonian. Higher levels of approximation are considered in the zero differential overlap (ZDO) approximation family of semiempirical Hamiltonians.[2−5] The complete neglect of differential overlap (CNDO) method does not include exchange two-electron integrals and will not be considered here. The intermediate neglect of differential overlap (INDO) which includes only one-center, two-electron exchange integrals, is considered in the parametrization labeled INDO/1. The neglect of differential diatomic overlap (NDDO) includes one-center and some two-center, two-electron exchange integrals. For this model, we consider three parametrizations labeled AM1, PM3, and MNDO. All of these methods include all valence electrons in the calculation, assume minimal basis sets for molecular orbitals comprised of linear combinations of atomic orbitals (LCAO-MO), and obtain the MOs through the Hartree−Fock self-consistent-field (SCF) method.

In this paper we evaluate these semiempirical Hamiltonians' performance using the shattering transition in the collision of C_{60} on a surface. The TB model has been employed to describe this phenomenon when the surface is modeled as well as the projectile in the MD simulation.[6,7] We include the TB Hamiltonian as a reference on the role of replacing the active surface with a passive surface. The ZDO Hamiltonians have the advantage that they more closely resemble the underlying full Hamiltonian and hence would be expected to yield better gradients when parametrized for a description of the interatomic potentials. Further, in the TB model the interactions between two atoms are represented by solely one-center parameters multiplied by general scaling factors that play the role of overlap integrals in Hückel theory which will present problems for the description of heterogeneous systems. As the ZDO approximation can be flexible enough to describe such systems with more complexity, it is likely to have advantages over the TB model for MD simulations involving differing types of atoms.

The use of ZDO Hamiltonians is a step toward ab initio theory where all two-electron integrals are fully calculated and electron correlation can be considered explicitly. The computational intensity of such calculations makes them impractical for the generation of forces for large scale MD simulations. Another first-principles approach to the driving of MD simulations is density functional theory, which is more applicable than ab initio correlated methods, but should be an order of magnitude slower than an NDDO description.

Many research efforts have addressed the C_{60} molecule and the related fullerenes. One of the properties that interests investigators is the stability of fullerene clusters during collisions for initial translational energies up to 120 eV, although there are experimental results which show that molecules can dissociate by surface induced dissociation (SID).[8−11] The distribu-

10.1021/jp011394z CCC: $20.00
Published on Web 06/29/2001

tion of the energy and the pattern of the fragmentation of C_{60} are of interest in many experimental as well as theoretical studies, with the hope that the mechanism of the dissociation can be understood. At collision energies in excess of 100 eV, fragmentation can be detected on a microsecond time scale after surface impact, and even-numbered fullerene fragments (C_{58}^+, C_{56}^+, C_{54}^+) are observed experimentally.[12] Studies have also shown that when the collision energy is higher than 300 eV, the fragmentation mechanism changes to a prompt catastrophic shattering at or near the surface on a subpicosecond time scale.[13]

To discern a possible mechanism for the C_{60} fragmentation, many molecular dynamics simulations have been done to study the collision of the C_{60} molecule and various surfaces, using forces from empirical potentials.[14,15] More recently, the tight-binding method has been employed to calculate the forces of the system.[6,7] Here, ZDO semiempirical methods are used to study the collision of the C_{60} molecule with a passive surface, i.e., one that provides only a repulsive interaction with the projectile. All of the ZDO-type Hamiltonians used here are designed to reproduce properties of large organic molecules, hence the carbon parameters are already fairly well optimized. As a first survey of these methods as drivers for MD simulations, we expect reasonable simulation results without further refinement. Obviously, we are always free to reparametrize such a Hamiltonian to fit ab initio derived forces, as has been done elsewhere.[16,17] These methods will be compared with each other and to the TB Hamiltonian to determine which of the semiempirical forms has the most promise for a reparametrization specific to the needs of MD simulation.

Computational Details

With the goal of evaluating the performance of ZDO Hamiltonians among themselves and with reference to the TB Hamiltonian,[18] we have used the INDO Hamiltonian from the ZINDO package,[19,20] and the NDDO Hamiltonians: AM1,[21] PM3,[22] and MNDO,[23] from MOPAC 6.0[24] in GAMESS.[25] All INDO and NDDO calculations are done using unrestricted Hartree−Fock (UHF) wave functions. Results for the TB simulation have been generated using the same time integration algorithms as those used for the ZDO Hamiltonians.

The passive surface is placed in the $x-y$ plane with the z-coordinate defined to be zero. The passive wall potential is written in Hartree atomic units as

$$V_i = V_0\{1 - \tanh(\gamma z_i)\} \tag{1}$$

where z_i is the distance between the ith atom and the surface, and V_i is the potential felt by the ith atom. We set $V_0 = 100$ Hartree, and $\gamma = 1.0$, so that the C_{60} molecule gradually feels the potential, and the potential is repulsive enough to prevent the C_{60} molecule from passing over the barrier. The projectile approaches the surface at an angle of 20° from the normal to the surface. While this causes an overall rotation of the molecule, the initial configuration is identical and the overall rotation should yield a similar face striking the passive surface to allow for the comparison of the various Hamiltonians.

We use the position-Verlet algorithm to generate the nuclear trajectories by numerically integrating Newton's equations of motion. Forces are calculated employing each of the five different Hamiltonians under consideration. Two initial kinetic energies are chosen: 100 eV, which is below the shattering regime, and 300 eV, which is in the shattering regime. Time step sizes are chosen to ensure that the integration proceeds well beyond the encounter of the molecule with the surface, yet small enough that the numerical integration does not introduce appreciable error into the calculation. The time step for the ZDO Hamiltonians is 5 au (40 au $\sim$ 1 fs), while a 10 au time step is used for the TB Hamiltonian when the impact energy is 100 eV. At the impact energy of 300 eV, smaller time steps are required for the ZDO Hamiltonians due to the more severe nature of the physical phenomena simulated. The dynamics of shattering encounters configurations that are far from equilibrium, and hence is more computationally demanding for the ZDO Hamiltonians. The step size varies from 0.1 au to 2.0 au, with the major concern being the convergence of the SCF during the electronic structure calculations. The TB Hamiltonian does not require an SCF procedure and the 10 au time step continues to be used. To facilitate the SCF convergence for ZDO Hamiltonians, the initial guess for the molecular orbitals at each new time is taken from the converged MOs of the previous time.

The initial configuration of the C_{60} molecule for the 100 eV collision has a pentagonal face approaching the wall potential. It is advantageous in the 300 eV collision to have a single bond facing the wall potential, as, when a pentagonal or hexagonal face is approaching the wall, multiple bond breaking leads to much greater difficulty in achieving SCF convergence. Data recorded during the simulations included molecular configurations, total kinetic energy, and center-of-mass kinetic energy, each as a function of time. The primary purpose of this study is to compare the results for ZDO Hamiltonians with the widely used TB Hamiltonian under the same initial simulation conditions. We use the computationally simple passive surface to ease the computational burden of this comparison. At higher incident energies, experimental results have been found on surfaces of graphite, passivated silicon, and tantalum[13] and we will compare some of our results to these.

Results

100 eV. The molecular dynamics simulations for all Hamiltonians are done for 1 ps of simulation time for collisions at 100 eV. At the final time, there was no evidence of fragmentation for any of the simulations, in agreement with what has been seen experimentally. We define the height of the molecule to be the largest magnitude difference in the z coordinate between any pair of carbon atoms. By this definition, the initial height of the molecule is 7.10 Å and diminishes to 3.17 Å at about 155 fs for the PM3 Hamiltonian; 3.23 Å at about 154 fs for MNDO; 3.28 Å at about 144 fs for TB; 3.37 Å at about 157 fs for AM1; and 3.62 Å at about 138 fs for INDO. We note that the NDDO-based Hamiltonians give minimum heights that are in good agreement with TB at roughly 10 fs later than TB. The INDO Hamiltonian is at substantial disagreement with the TB result and is the only ZDO Hamiltonian that finds the minimum height before TB.

With the exception of the INDO Hamiltonian, the C_{60} molecule retains the cage and oscillates around the familiar "soccer ball" shape after the collision with the passive surface. In the case of the INDO Hamiltonian, the molecule never regains its original shape, but rather, many 3- and 4-membered rings are formed after the collision. Such enhanced stability of ring forms in INDO methods is well-known.

In Figure 1, the longest width of the projection of the ball onto the plane of the surface is presented as a function of the simulation time. The second plot is for the TB Hamiltonian and shows an initial increase in this dimension as the molecule

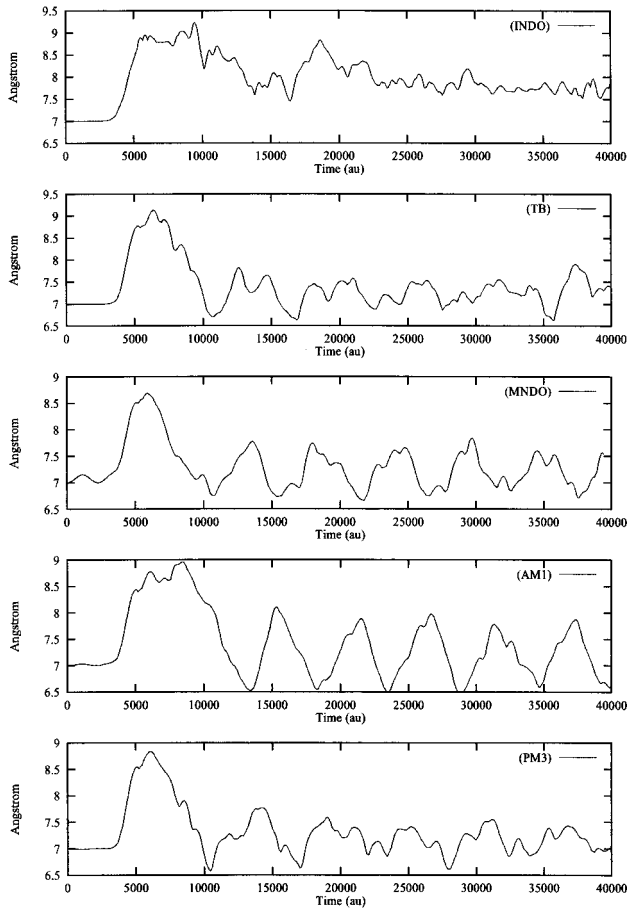

Figure 1. Long axis of the C_{60}, projected on surface, in Å vs time (au) (100 eV).

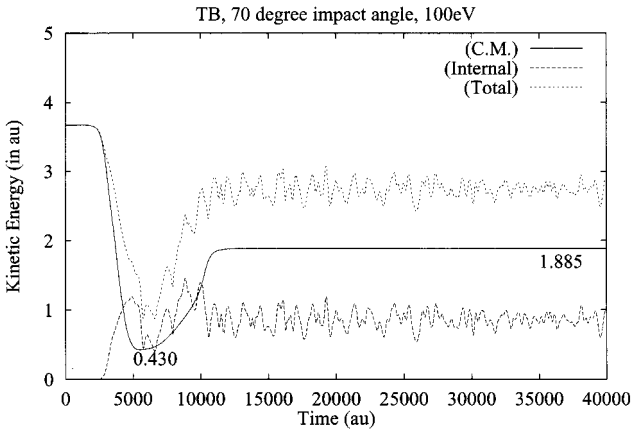

Figure 2. Kinetic energies as a function of time in au, TB (100 eV).

impacts the surface. At later times, the longest width of this projection shows a complicated set of oscillations that are indicative of the excitation of a number of vibrations in the molecule and this persists to the final simulation time. The NDDO-based Hamiltonians display a similar behavior as a function of time indicating that they drive a similar molecular dynamics simulation. Again, the INDO Hamiltonian yields results that differ from the other four Hamiltonians, after the impact with the surface, at late times, this Hamiltonian leads to a larger dimension with less pronounced oscillation.

The total kinetic energy, center-of-mass kinetic energy, and their difference, the internal kinetic energy, are shown in Figures 2−6 as functions of time. The two numbers in each plot correspond to the center-of-mass kinetic energies at two points

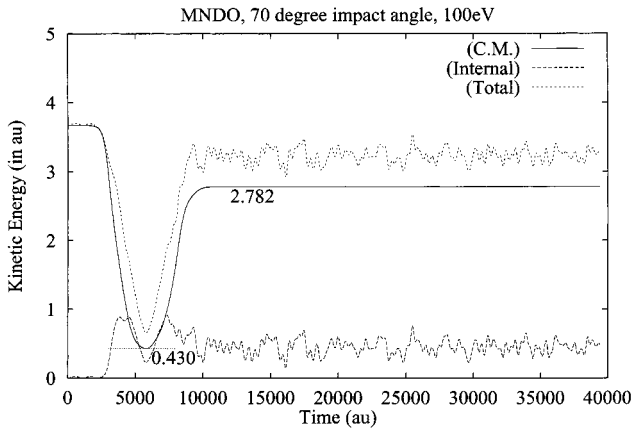

Figure 3. Kinetic energies as a function of time in au, MNDO (100 eV).

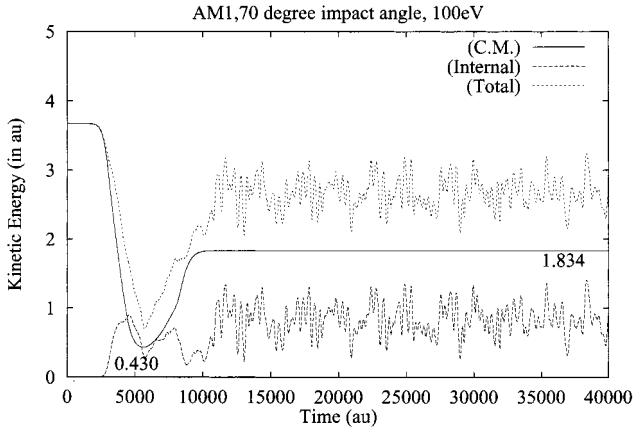

Figure 4. Kinetic energies as a function of time in au, AM1 (100 eV).

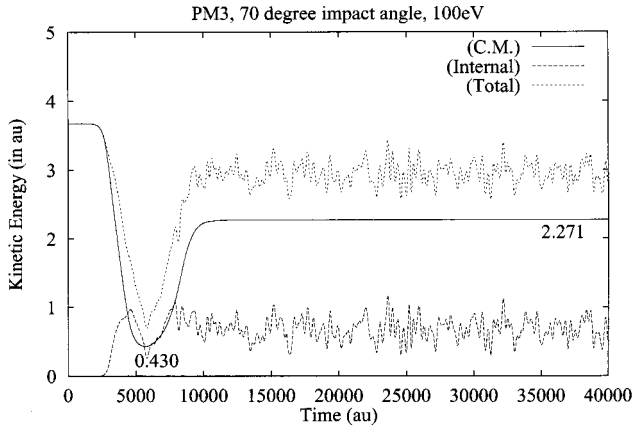

Figure 5. Kinetic energies as a function of time in au, PM3 (100 eV).

in time. The minimum center-of-mass kinetic energy is realized when the sum of the *z*-direction velocities becomes zero, near or at the total kinetic energy minimum. The final center-of-mass kinetic energy is realized when the cluster experiences zero potential from the surface, near the end of the simulation. Table 1 shows the center-of-mass kinetic energy and the percentage of the initial energy that it represents at the end of the simulations for the 100 eV impact. The TB simulation finds that the final center-of-mass kinetic energy is roughly half the initial energy for this collision configuration. Two of the three NDDO based Hamiltonians, AM1 and PM3, yield slightly less and slightly more final center-of-mass kinetic energies, respectively. The MNDO simulation shows a rather larger final value

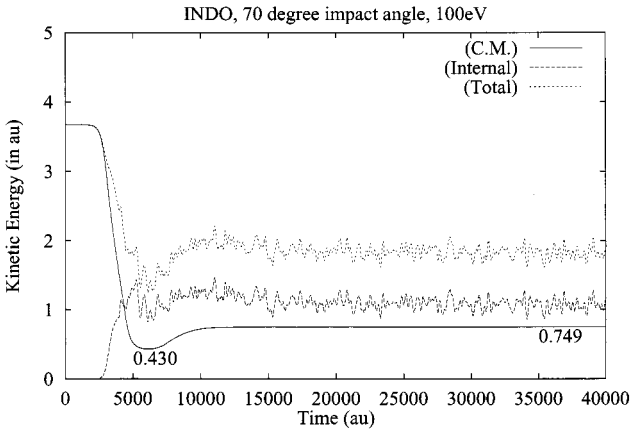

Figure 6. Kinetic energies as a function of time in au, INDO (100 eV).

TABLE 1: Final Center-of-Mass, E_{kin}^{cm} and Internal, E_{kin}^{in} Kinetic Energies for 100 eV Projectile in Au

	AM1	PM3	MNDO	INDO	TB
E_{kin}^{cm}	1.834	2.271	2.782	0.749	1.897
E_{kin}^{in}	0.834	0.683	0.453	1.088	0.860
E_{kin}^{cm}/E_i (%)	49.9%	61.8%	75.7%	20.4%	51.6%

than any of the TB, AM1, and PM3 results. Finally, the INDO Hamiltonian yields the only final center-of-mass kinetic energy that is substantially less than half the initial energy and this seems to be an additional confirmation of the poor quality of the INDO approximation for driving this sort of MD simulation.

300 eV. Obtaining SCF convergence for the INDO and NDDO Hamiltonians is more challenging at the higher energy because of the amount of bond breaking that is seen in the simulation. As a result of this computationally demanding requirement, simulations at the 300 eV impact energies are limited to somewhat shorter simulation times. However, each simulation is run to, at least, 500 fs at which time the interactions between the atoms that comprise the initial molecule and the passive surface cease.

Figure 7 presents the configuration of the C_{60} molecule, projected onto the plane of the surface, after about 200 fs of simulation time, the impact with the surface peaked before 100 fs, when driven by TB. The impact energy of 300 eV is above the threshold for shattering of the molecule and shattering is seen in this simulation. TB gives the most (and smallest) fragments of all the Hamiltonians here considered. There are 4 single atoms farther than a bonding distance from the rest of the molecule, as well as 4 diatomic fragments, 6 triatomic fragments, and one each of 4-, 5-, 8-, and 13-member fragments. Figure 8 presents the same time configuration for the AM1-driven simulation. At this time, the simulation shows one monatomic and one triatomic fragment separated from the main body of the projectile molecule, which is still intact. AM1 shows the least fragmentation of the NDDO Hamiltonians. Figure 9 shows the PM3 results which show three triatomic fragments, as well as single fragments comprised of 1, 5, 10, and 35 atoms, while Figure 10 shows single fragments of 2, 3, 4, 6, and 45 atoms for the MNDO parametrization. Again, the INDO simulation, Figure 11, shows a degree of binding that is greater than any of the others, with the molecule still intact, though distorted, after 200 fs of simulation.

We note that the shattering of the molecule from a passive surface using TB and NDDO Hamiltonians is in qualitative agreement with previous TB simulations of C_{60} on a reconstructed diamond surface[7] as a function of the collision energy. At the lower energy, there is no fragmentation during the simulation, while at the higher energy, carbon chains are formed after the collision, a phenomenon also reported in a study of the melting of fullerenes.[15]

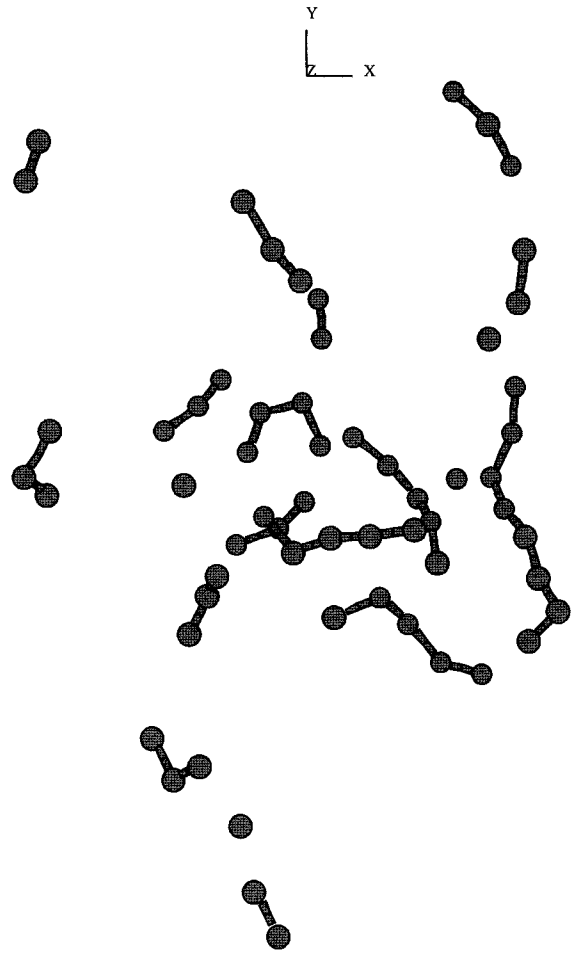

Figure 7. Snapshot at $t \sim 200$ fs, TB (300 eV).

The total kinetic energy, center-of-mass kinetic energy, and their difference, the internal kinetic energy, are shown in Figures 12−16 as functions of time. As with the 100 eV projectile, the two numbers in each plot correspond to the kinetic energies at two points in time. The smaller kinetic energy is realized when the sum of the *z*-direction velocities becomes zero, near or at the kinetic energy minimum. The larger kinetic energy is realized when the cluster experiences zero potential from the surface, near the end of the simulation. Table 2 displays the average internal kinetic energy and the center-of-mass kinetic energy at the end of the 300 eV projectile simulations. The original configuration for the 300 eV simulations is different from the original configuration for the 100 eV case, so that comparisons between the two energies are not on equal footing, however they may still be suggestive. First, we note that the center-of-mass kinetic energy is a smaller percentage of the initial energy than was the case for the lower projectile energy for each of the five Hamiltonians considered. In fact, the final center-of-mass kinetic energy is less for the higher projectile energy than for the lower projectile energy in the case of both the PM3 and the MNDO Hamiltonians. The INDO Hamiltonian shows the greatest increase in center-of-mass kinetic energy with impact energy followed by the TB simulation. Again, the nature of the passive surface considered rules out the direct comparison of our calculated results to those of experiment.

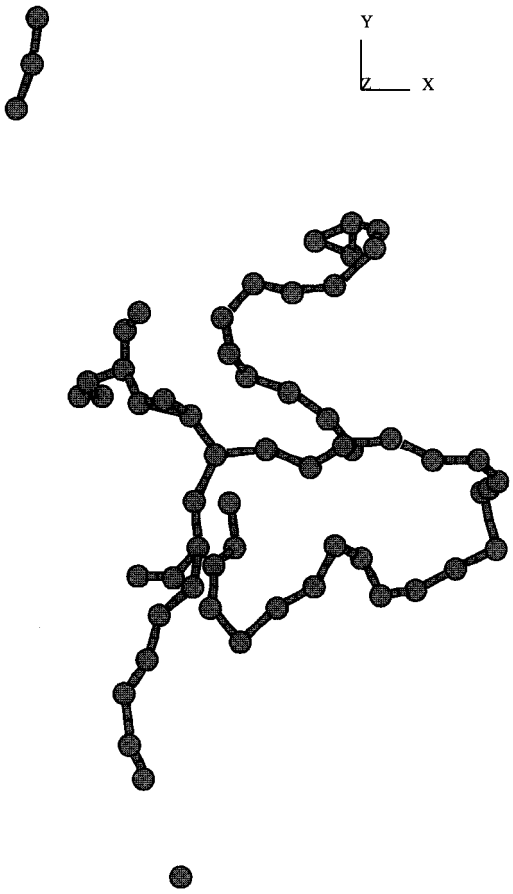

Figure 8. Snapshot at $t \sim 200$ fs, AM1 (300 eV).

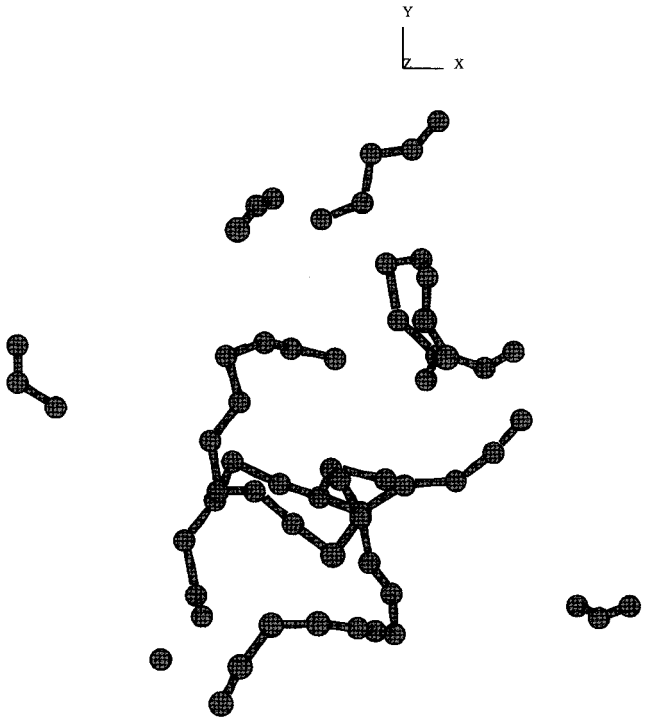

Figure 9. Snapshot at $t \sim 200$ fs, PM3 (300 eV).

These results concerning the final center-of-mass kinetic energy are in qualitative agreement with those of Blaudeck et al.[6] They find that the final center-of-mass kinetic energy is either independent of the initial projectile energy or decreases as the projectile energy increases. We arrive at a final value of this kinetic energy that is a good deal greater than theirs. This may be due to either the fact that we only consider one initial configuration, or that we use a passive surface that is incapable of absorbing any of the impact energy, or both. It is clear from our calculations that the fraction of the initial kinetic energy that becomes final center-of-mass energy is a decreasing fraction as the projectile energy increases.

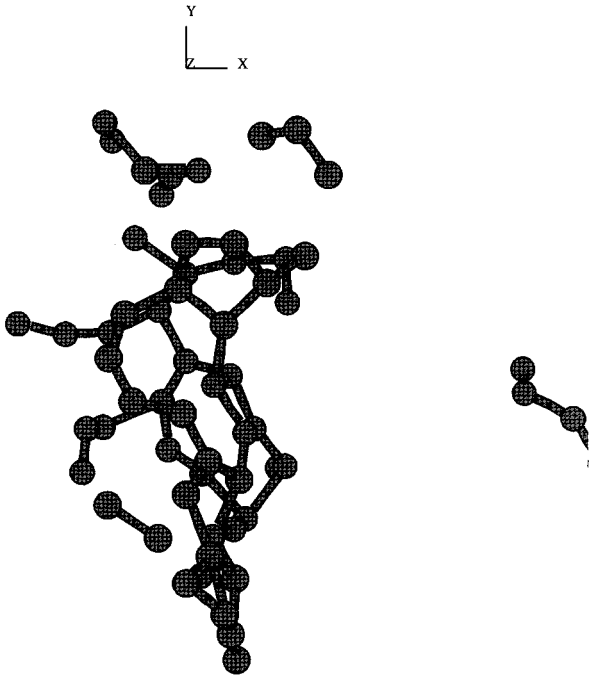

Figure 10. Snapshot at $t \sim 200$ fs, MNDO (300 eV).

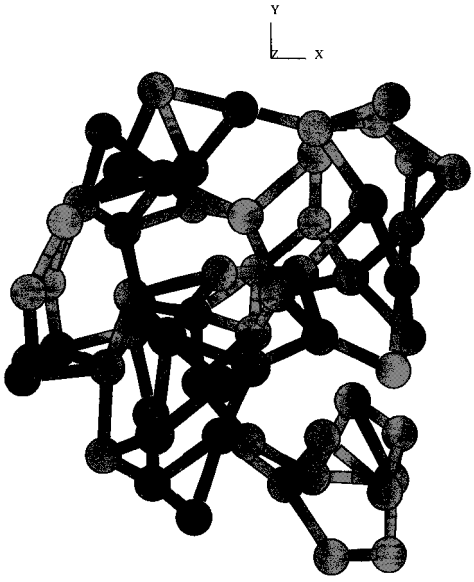

Figure 11. Snapshot at $t \sim 200$ fs, INDO (300 eV).

The difficulty experienced for the SCF convergence of the ZDO Hamiltonians is indicative of the complexity of the physical phenomena involved in the collision at the higher collision energy. The onset of bond breaking suggests that a number of excited states have become important for the realistic calculation of the MD forces. In this regard, the TB Hamiltonian does not include any excited-state effects while the NDDO Hamiltonians can incorporate some of these effects in an approximate way, though the present treatment does not. It would appear that a future reparametrization of the NDDO Hamiltonian based on high level ab initio results may produce more realistic forces for MD simulations.

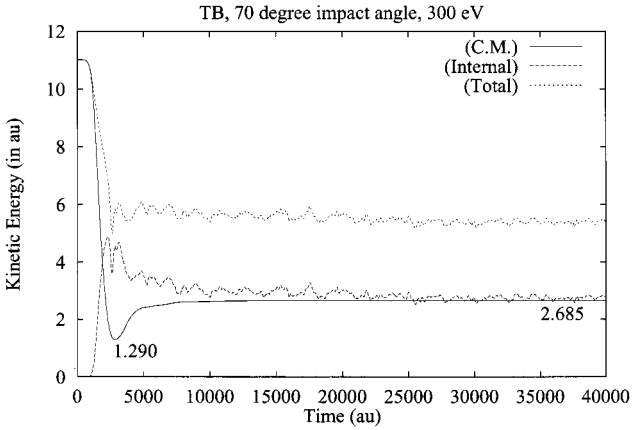

Figure 12. Kinetic energies as a function of time in au, TB (300 eV).

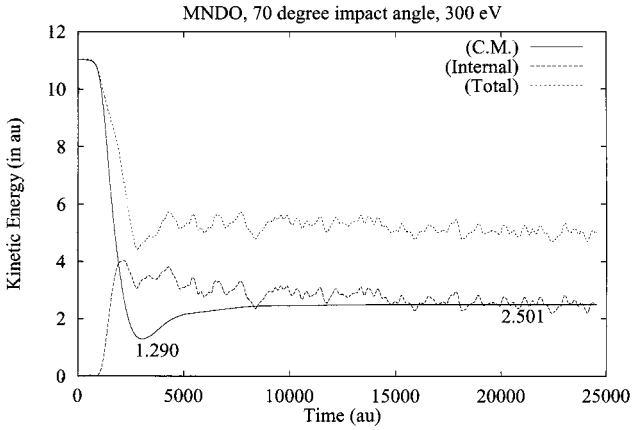

Figure 13. Kinetic energies as a function of time in au, MNDO (300 eV.)

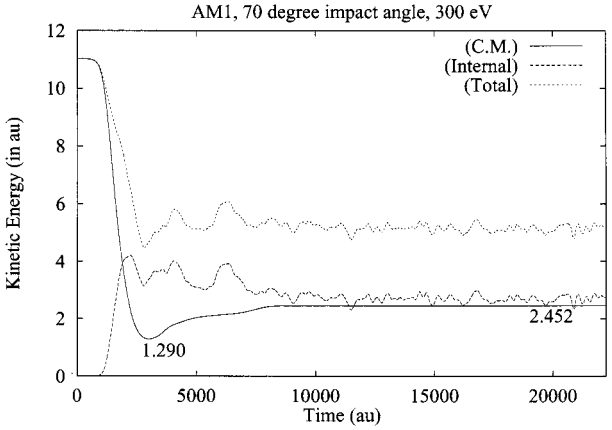

Figure 14. Kinetic energies as a function of time in au, AM1 (300 eV).

Conclusions

We compare the use of four ZDO Hamiltonians, with the TB Hamiltonian, for the direct MD simulation of the C_{60} molecule colliding with a passive surface. The TB Hamiltonian was designed for direct MD simulations while the four ZDO Hamiltonians have been parametrized for use in electronic structure calculations. The collision is studied at two impact energies, 100 eV, which is below the shattering regime and 300 eV, which is in the shattering regime. After one picosecond of simulation time, there is no evidence of fragmentation for the simulation at the lower energy from any of the Hamiltonians considered. At the higher energy, the TB and all three NDDO

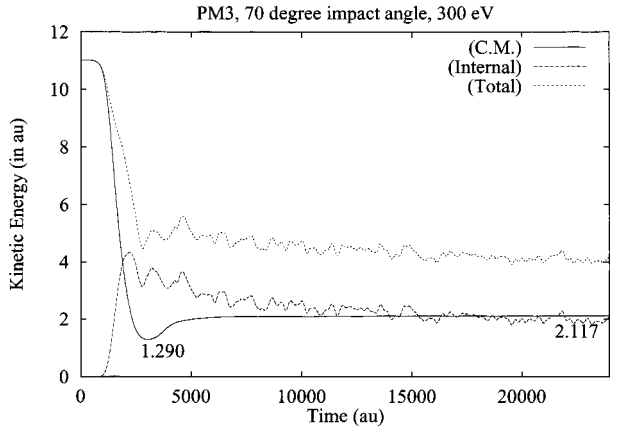

Figure 15. Kinetic energies as a function of time in au, PM3 (300 eV).

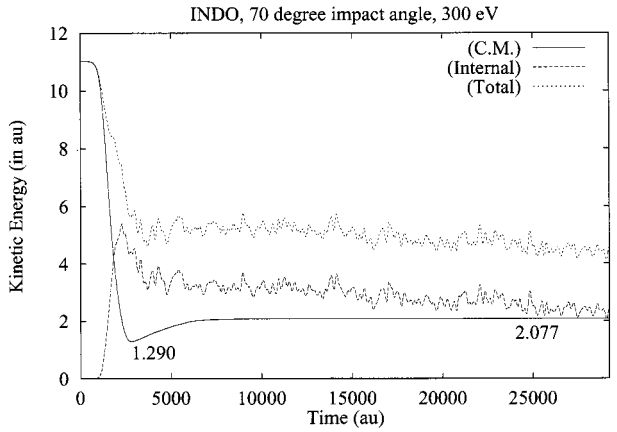

Figure 16. Kinetic energies as a function of time in au, INDO (300 eV).

TABLE 2: Final Center-of-Mass, E_{kin}^{cm} and Internal, E_{kin}^{in} Kinetic Energies for 300 eV Projectile in Au

	AM1	PM3	MNDO	INDO	TB
E_{kin}^{cm}	2.452	2.117	2.501	2.077	2.685
E_{kin}^{in}	2.701	2.030	2.555	2.637	2.804
E_{kin}^{cm}/E_i (%)	22.2%	19.2%	22.7%	18.8%	24.4%

simulations showed significant fragmentation after 200 fs of simulation time. These results are in qualitative agreement with both experimental[13] and theoretical[7,15] studies. The INDO Hamiltonian showed no such fragmentation in the higher energy simulation.

The partitioning of the initial kinetic energy into center-of-mass kinetic energy and internal energy is different at the two impact energies. The percentage of the initial kinetic energy that is realized as final center-of-mass kinetic energy is less for greater impact energy. This behavior is seen by all five Hamiltonians, however, the INDO simulation shows a markedly smaller percentage at the lower collision energy than any of the other four simulations. As we have considered only one initial configuration for each energy, no conclusions about the quantitative behavior of these simulations in comparison to experiment, seems justified.

By comparison to the TB Hamiltonian, the three NDDO Hamiltonians, AM1, PM3, and MNDO, seem to give reasonable qualitative agreement for these simulations. The NDDO Hamiltonians have not been specifically parametrized for MD and so we anticipate that reparametrization of the NDDO form may well lead to superior performance in providing input to MD

simulations. It appears from our results that the INDO Hamiltonian does not preserve enough of the chemical information necessary for such simulations. The difficult SCF convergence at the higher impact energy is an indication that more than one electronic state is involved in the process that leads to fragmentation, as would be assumed in bond breaking. The TB Hamiltonian is not expected to perform well for the multiple bond breaking involved in the fragmentation process at the higher impact energy. The NDDO form also has the advantage that the inclusion of heteroatoms in the simulation follows naturally without the need to introduce the other scaling factors that would be required by the TB Hamiltonian.

The NDDO Hamiltonians used here are parametrized for molecules in their ground electronic state. To use this form for practical MD simulations, it is necessary to reparametrize with an emphasis on the description of the bonding of the systems considered, which may lead to easier SCF convergence. The reparametrization will need to include molecular properties corresponding not only to the ground electronic state, but also low lying excited states in an average way. Molecular properties obtained from high level ab initio post Hartree−Fock methods, such as coupled-cluster or configuration interaction methods can be used to guide the generation of new NDDO parameters. From this study, it appears that the NDDO form has sufficient complexity to accommodate MD simulations that lead to configurations far away from equilibrium.

Acknowledgment. The authors thank Drs. M. Hedström and F. Harris for their helpful critiques throughout this work. This work is support by NSF Grant No. DMR 9980015.

References and Notes

(1) Hückel, E. P. *Z. Physik* **1931**, *70*, 204.
(2) Pople, J. A.; Segal, G. A. *J. Chem. Phys*. **1965**, *43*, S136.
(3) Pople, J. A.; Segal, G. A. *J. Chem. Phys*. **1966**, *44*, 3289.
(4) Pople, J. A.; Beveridge, D. L.; Dobosh, P. A. *J. Chem. Phys*. **1967**, *47*, 2026.
(5) Santry, D. P.; Segal, G. A. *J. Chem. Phys*. **1967**, *47*, 158.
(6) Blaudeck, P.; Frauenheim, T.; Busmann, H.-G.; Lill, T. *Phys. Rev. B* **1994**, *49*, 11409.
(7) Galli, G.; Mauri, F. *Phys. Rev. Lett*. **1994**, *73*, 3471.
(8) Eckstein, W.; Verbeck, H.; Datz, S. *Appl. Phys. Lett*. **1975**, *27*, 527.
(9) Heiland, W.; Taflauer, E. *Nucl. Instrum. Methods* **1982**, *194*, 667.
(10) Cooks, R. G.; Ast, T.; Beynon, J. H. *Int. J. Mass Spectrom. Ion Proc*. **1975**, *16*, 348.
(11) Gandy, R. M.; Ampulaski, R.; Prusaczyk, J.; Johnson, R. H. *Int. J. Mass Spectrom. Ion. Phys*. **1977**, *24*, 363.
(12) Beck, R. D.; Weis, P.; Rockenberger, J.; Kappes, M. M. *J. Chem. Phys*. **1996**, *104*, 3638.
(13) Beck, R. D.; Warth, C.; May, K.; Kappes, M. M. *Chem. Phys. Lett*. **1996**, *257*, 557.
(14) Mowrey, R. C.; Brenner, D. W.; Dunlap, B. I.; Mintmire, J. W.; White, C. T. *J. Phys. Chem*. **1991**, *95*, 7138.
(15) Kim, S. G.; Tománek, D. *Phys. Rev. Lett*. **1994**, *72*, 2418.
(16) (a) Gonzalez-Lafont, A.; Truong, T. N.; Truhlar, D. G. *J. Phys. Chem*. **1991**, *95*, 4618. (b) Liu, Y.-P.; Lynch, G. C.; Truong, T. N.; Lu, D.-H.; Truhlar, D. G.; Garrett, B. C. *J. Am. Chem. Soc*. **1993**, *115*, 2408. (c) Rossi, I.; Truhlar, D. G. *Chem. Phys. Lett*. **1995**, *233*, 231. (d) Corchado, J. C.; Truhlar, D. G. In *Combined Quantum Mechanical and Molecular Mechanical Methods*; Gao, J., Thompson, M. A., Eds.; ACS Symposium Series, American Chemical Society: Washington, DC, 1998; Vol. 712, p 106. (e) Chuang, Y.-Y.; Radhakrishnan, M. L.; Fast, P. L.; Cramer, C. J.; Truhlar, D. G. *J. Phys. Chem. A* **1999**, *103*, 4893.
(17) Runge, K.; Cory, M. G.; Bartlett, R. J. *J. Chem. Phys*. **2001**, *114*, 5141.
(18) Xu, C. H.; Wang, C. Z.; Chan, C. T.; Ho, K. M. *J. Phys: Condens. Matter* **1992**, *4*, 6047.
(19) Ridley, J.; Zerner, M. C. *Theor. Chim. Acta* **1973**, *32*, 111.
(20) Ridley, J.; Zerner, M. C. *Theor. Chim. Acta* **1976**, *42*, 223.
(21) Dewar, M. J. S.; Zoebisch, E. G.; Healy, E. F.; Stewart, J. J. P. *J. Am. Chem. Soc*. **1985**, *107*, 3902.
(22) Stewart, J. J. P. *J. Comput. Chem*. **1989**, *10*, 209, 221.
(23) Dewar, M. J. S.; Thiel, W. *J. Am. Chem. Soc*. **1977**, *99*, 4899.
(24) Stewart, J. J. P. *J. Comput.-Aided Mol. Des*. **1990**, *4*, 1.
(25) Schmidt, M. W.; Baldridge, K. K.; Boatz, J. A.; Elbert, S. T.; Gordon, M. S.; Jensen, J. H.; Koseki, S.; Matsunaga, N.; Nguyen, K. A.; Su, S. J.; Windus, T. L.; Dupuis, M.; Montgomery, J. A. *J. Comput. Chem*. **1993**, *14*, 1347.